

NUMERICAL ANALYSIS AND SCIENTIFIC COMPUTING
PREPRINT SERIA

**On the sensitivity to the filtering radius in
Leray models of incompressible flow**

L. BERTAGNA A. QUAINI L. G. REBHOLZ A. VENEZIANI

PREPRINT #53



DEPARTMENT OF MATHEMATICS
UNIVERSITY OF HOUSTON

JUNE 2016

On the sensitivity to the filtering radius in Leray models of incompressible flow

Luca Bertagna, Annalisa Quaini, Leo G. Rebholz and Alessandro Veneziani

Abstract One critical aspect of Leray models for the Large Eddy Simulation (LES) of incompressible flows at moderately large Reynolds number (in the range of few thousands) is the selection of the filter radius. This drives the effective regularization of the filtering procedure, and its selection is a trade-off between stability (the larger, the better) and accuracy (the smaller, the better). In this paper, we consider the classical Leray- α and a recently introduced (by one of the authors) Leray model with a deconvolution-based indicator function, called Leray- α -NL. We investigate the sensitivity of the solutions to the filter radius by introducing the sensitivity systems, analyzing them at the continuous and discrete levels, and numerically testing them on two benchmark problems.

1 Introduction

The Direct Numerical Simulation (DNS) of the Navier-Stokes equations (NSE) computes the evolution of all the significant flow structures by resolving them with a properly refined mesh. Unfortunately, when convection dominates the dynamics

Luca Bertagna
Department of Scientific Computing, Florida State University, Tallahassee (FL) USA, e-mail: lbertagna@fsu.edu

Annalisa Quaini
Department of Mathematics, University of Houston, Houston (TX) USA, e-mail: quaini@math.uh.edu

Leo G. Rebholz
Department of Mathematical Sciences, Clemson University, Clemson (SC) USA, e-mail: rebholz@clemson.edu

Alessandro Veneziani
Department of Mathematics and Computer Science, Emory University, Atlanta (GA) USA, e-mail: ale@mathcs.emory.edu

- which happens in many practical applications - this requires very fine meshes, making DNS computationally unaffordable for practical purposes. A possible way to limit the computational costs associated with DNS without sacrificing accuracy is to solve for the flow average, and model properly the effects of the (not directly solved for) small scales on the (resolved) larger scales.

The Leray- α model (1-4) has emerged as a useful model for turbulent flow predictions, thanks to the seminal work of Guerts, Holm, Titi and co-workers [15, 14, 13, 11] in the early-mid 2000's. The name of the model was given by Titi to honor Leray, who used a similar model in 1934 as a theoretical tool to help in understanding the well-posedness problem of the NSE [31]. The Leray- α model in [31] describes the small scale effects by a set of equations to be added to the discrete NSE formulated on the under-refined mesh. It was shown in [15, 14, 13, 11] that the Leray- α model is well-posed, it can accurately predict turbulent flow on the large scales, where it preserves Kolmogorov's $-5/3$ law. Moreover, the model can accurately predict the boundary layer. Over the last decade, much more theoretical and computational work has been done to the Leray- α model and several variations of it [38, 17, 18, 32, 23, 29, 19, 10, 33, 6, 2], most of which gives further evidence of the usefulness of the model as an effective tool for coarse-mesh predictions of higher Reynolds number flow.

The filtering radius α plays a central role in the Leray- α model, and Leray type models in general, since it determines the amount of regularization to apply. In particular, larger values lead to more regularized solutions, while for $\alpha = 0$, the models reduce to the NSE; see (1-4) below. Our interest herein is to understand how solutions of the classical Leray- α model and one possible generalization, called Leray- α -NL, depend on α . Parameter sensitivity investigations in fluid flow problems are critical in understanding the reliability of computed solutions [1, 34, 21, 36, 37, 3, 4, 16, 5]. However, it is often prohibitively costly to identify the appropriate value by running many computations with different choices, especially when the flow problems require fine meshes. An attractive alternative is the sensitivity equation method that computes explicitly the derivative of the solution with respect to the parameter. This system can then be solved simultaneously with the model at each time step of the simulation. Depending on the specific model, the solution of the sensitivity system may be challenging, and its analysis and efficient discretization design require specific investigation. This is exactly the purpose of this paper for the two models of choice.

The outline of the paper is as follows. In Sec. 2 we introduce the continuous Leray- α and Leray- α -NL models and derive the corresponding sensitivity equations. In Sec. 3 we propose efficient and stable numerical schemes for the approximation of both models and their sensitivity systems. Finally, in Sec. 4 we test the proposed numerical schemes against two benchmark problems. Conclusions are drawn in Sec. 5.

2 Problem definition

We consider a spacial domain $\Omega \subset \mathbb{R}^d$ ($d = 2$ or 3) and time interval $(0, T)$, with $T > 0$. The classical Leray- α model takes the form:

$$\mathbf{u}_t + \bar{\mathbf{u}} \cdot \nabla \mathbf{u} + \nabla p - \nu \Delta \mathbf{u} = \mathbf{f} \quad \text{in } \Omega \times (0, T), \quad (1)$$

$$\nabla \cdot \mathbf{u} = 0 \quad \text{in } \Omega \times (0, T), \quad (2)$$

$$\nabla \lambda - \alpha^2 \Delta \bar{\mathbf{u}} + \bar{\mathbf{u}} = \mathbf{u} \quad \text{in } \Omega \times (0, T), \quad (3)$$

$$\nabla \cdot \bar{\mathbf{u}} = 0 \quad \text{in } \Omega \times (0, T), \quad (4)$$

endowed with suitable boundary conditions, e.g.:

$$\mathbf{u} = \bar{\mathbf{u}} = \mathbf{u}_{in} \quad \text{on } \Gamma_{in} \times (0, T), \quad (5)$$

$$\mathbf{u} = \bar{\mathbf{u}} = \mathbf{0} \quad \text{on } \Gamma_{wall} \times (0, T), \quad (6)$$

$$(\nu \nabla \mathbf{u} - pI) \cdot \mathbf{n} = (\alpha^2 \nabla \bar{\mathbf{u}} - \lambda I) \cdot \mathbf{n} = \mathbf{0} \quad \text{on } \Gamma_{out} \times (0, T), \quad (7)$$

and initial condition $\mathbf{u} = \mathbf{u}_0$ in $\Omega \times \{0\}$. In (1-7), \mathbf{u} represents the fluid velocity (which is considered ‘‘averaged’’ in some sense), p the fluid pressure, $\nu > 0$ the kinematic viscosity, \mathbf{f} a body force, and \mathbf{u}_{in} and \mathbf{u}_0 are given. The equations (3,4) represent the α -filter applied to \mathbf{u} , where $\bar{\mathbf{u}}$ is the resulting filtered variable and $\alpha > 0$ is the filtering radius. This is the radius of the neighborhood where the filter extracts information from the unresolved scales. The Lagrange multiplier λ is necessary to enforce a solenoidal $\bar{\mathbf{u}}$ in non-periodic flows. The inlet and outlet sections are denoted by Γ_{in} and Γ_{out} , while Γ_{wall} is the rest of the boundary. We note that the correct boundary conditions for $\bar{\mathbf{u}}$ on solid walls is unsettled in the LES community, although the computational experience of the authors is that a no-slip condition generally produces good results.

We also consider also the following generalized version of the Leray- α model, proposed in [7]:

$$\mathbf{u}_t + \tilde{\mathbf{u}} \cdot \nabla \mathbf{u} + \nabla p - \nu \Delta \mathbf{u} = \mathbf{f} \quad \text{in } \Omega \times (0, T), \quad (8)$$

$$\nabla \cdot \mathbf{u} = 0 \quad \text{in } \Omega \times (0, T), \quad (9)$$

$$\nabla \lambda - \alpha^2 \nabla \cdot (a(\mathbf{u}) \nabla \tilde{\mathbf{u}}) + \tilde{\mathbf{u}} = \mathbf{u} \quad \text{in } \Omega \times (0, T), \quad (10)$$

$$\nabla \cdot \tilde{\mathbf{u}} = 0 \quad \text{in } \Omega \times (0, T), \quad (11)$$

endowed with boundary conditions

$$\mathbf{u} = \tilde{\mathbf{u}} = \mathbf{u}_{in} \quad \text{on } \Gamma_{in} \times (0, T), \quad (12)$$

$$\mathbf{u} = \tilde{\mathbf{u}} = \mathbf{0} \quad \text{on } \Gamma_{wall} \times (0, T), \quad (13)$$

$$(\nu \nabla \mathbf{u} - pI) \cdot \mathbf{n} = (\alpha^2 a(\mathbf{u}) \nabla \tilde{\mathbf{u}} - \lambda I) \cdot \mathbf{n} = \mathbf{0} \quad \text{on } \Gamma_{out} \times (0, T). \quad (14)$$

The scalar function $a(\mathbf{u})$, called the *indicator function*, is crucial for the success of model (8-11), and satisfies:

$a(\mathbf{u}) \simeq 0$ where the velocity \mathbf{u} does not need regularization,
 $a(\mathbf{u}) \simeq 1$ where the velocity \mathbf{u} does need regularization,

so to detect the regions of the domain where regularization is needed. Notice that the choice $a(\mathbf{u}) = 1$ in (8-11) corresponds to system (3,4). In fact, in this way the operator in the filter equations is linear and constant in time, however its effectivity is rather limited, since it introduces the same amount of regularization in every region of the domain, hence causing overdiffusion in those region where the flow is already smooth.

Different choices of $a(\cdot)$ have been proposed and compared in [7, 6, 30, 28]. Here, we focus on a class of deconvolution-based indicator functions:

$$a(\mathbf{u}) = a_D(\mathbf{u}) = |\mathbf{u} - D(F(\mathbf{u}))|^2, \quad (15)$$

where F is a linear filter (an invertible, self-adjoint, compact operator from a Hilbert space to itself) and D is a bounded regularized approximation of F^{-1} . A popular choice for D is the Van Cittert deconvolution operator D_N , defined as

$$D_N = \sum_{n=0}^N (I - F)^n.$$

The evaluation of a_D with $D = D_N$ (deconvolution of order N) requires then to apply the filter F a total of $N + 1$ times. Since F^{-1} is not bounded, in practice N is chosen to be small, as the result of a trade-off between accuracy (for a regular solution) and filtering (for a non-regular one). In this paper, we consider $N = 0$, corresponding to $D_0 = I$. Numerical tests for $N = 1$ are considered for instance in [2].

We select F to be the linear Helmholtz filter operator F_H defined by

$$F = F_H = (I - \alpha^2 \Delta)^{-1}.$$

It is possible to prove [12] that

$$\mathbf{u} - D_N(F_H(\mathbf{u})) = (-1)^{N+1} \delta^{2N+2} \Delta^{N+1} F_H^{N+1} \mathbf{u}.$$

Therefore, $a_{D_N}(\mathbf{u})$ is close to zero in the regions of the domain where \mathbf{u} is smooth. Let us set $\hat{\mathbf{u}} = F_H(\mathbf{u})$. With $D = D_0$ and $F = F_H$, the indicator function (15) reads

$$a_{D_0}(\mathbf{u}) = |\mathbf{u} - \hat{\mathbf{u}}|^2. \quad (16)$$

System (8-11) with indicator function given by (16) is what we have called previously Leray- α -NL.

2.1 Sensitivity equation for Leray- α

Let us define

$$\mathbf{s} := \frac{\partial \mathbf{u}}{\partial \alpha}, \quad \mathbf{r} := \frac{\partial \bar{\mathbf{u}}}{\partial \alpha}, \quad \phi := \frac{\partial p}{\partial \alpha}, \quad \psi := \frac{\partial \lambda}{\partial \alpha}.$$

We develop the Leray- α sensitivity equation by differentiating model (1-4) with respect to α :

$$\mathbf{s}_t + \mathbf{r} \cdot \nabla \mathbf{u} + \bar{\mathbf{u}} \cdot \nabla \mathbf{s} + \nabla \phi - \nu \Delta \mathbf{s} = \mathbf{0} \quad \text{in } \Omega \times (0, T), \quad (17)$$

$$\nabla \cdot \mathbf{s} = 0 \quad \text{in } \Omega \times (0, T), \quad (18)$$

$$\nabla \psi - \alpha^2 \Delta \mathbf{r} + \mathbf{r} - \mathbf{s} = 2\alpha \Delta \bar{\mathbf{u}} \quad \text{in } \Omega \times (0, T), \quad (19)$$

$$\nabla \cdot \mathbf{r} = 0 \quad \text{in } \Omega \times (0, T). \quad (20)$$

System (17-20) is supplemented with boundary conditions:

$$\mathbf{s} = \mathbf{r} = \mathbf{0} \quad \text{on } \Gamma_{in} \cup \Gamma_{wall} \times (0, T), \quad (21)$$

$$(\nu \nabla \mathbf{s} - \phi \mathbf{I}) \cdot \mathbf{n} = \mathbf{0} \quad \text{on } \Gamma_{out} \times (0, T), \quad (22)$$

$$(\alpha^2 \nabla \mathbf{r} - \psi \mathbf{I}) \cdot \mathbf{n} = -2\alpha \nabla \bar{\mathbf{u}} \quad \text{on } \Gamma_{out} \times (0, T), \quad (23)$$

and initial condition $\mathbf{s} = \mathbf{0}$ in $\Omega \times \{0\}$. It is important to note that $\bar{\mathbf{s}} \neq \mathbf{r}$, i.e. filtering does not commute with differentiation in α . In addition, for both \mathbf{s} and \mathbf{r} we have homogeneous Dirichlet conditions at the inlet section and on the walls.

Sensitivity system (17-20) is a new system of partial differential equations, and thus it is important to consider its well-posedness. Its similarity to NSE and Leray models limits our well-posedness study to the case of periodic boundary conditions. Although this setting is typically not physically meaningful, we argue that a lack of well posedness for (17-20) with periodic boundary conditions would prevent a successful analysis for physical conditions such as (21-23).

The following result is promptly deduced from [11].

Lemma 1. *Suppose $\alpha > 0$, $\mathbf{f} \in L^2(0, T; L^2(\Omega)^d)$ and $\mathbf{u}_0 \in H^1(\Omega)^d$. Then the Leray- α model (1-4) equipped with periodic boundary conditions has a unique weak solution with $\mathbf{u} \in L^\infty(0, T; H^1(\Omega)^d) \cap L^2(0, T; H^2(\Omega)^d)$.*

Using this lemma, we can prove that system (17-20) with periodic boundary conditions is well-posed.

Theorem 1. *Under the assumptions of Lemma 1, the system (17-20) has a unique weak solution satisfying $\mathbf{s}, \mathbf{r} \in L^\infty(0, T; H^1(\Omega)^d) \cap L^2(0, T; H^2(\Omega)^d)$.*

Proof. The proof of this theorem follows standard arguments, since the sensitivity system is linear, and the smoothness assumptions of the data yield a sufficiently smooth velocity \mathbf{u} and filtered velocity $\bar{\mathbf{u}}$. \square

2.2 Sensitivity equation for Leray- α -NL

We define:

$$\mathbf{s} := \frac{\partial \mathbf{u}}{\partial \alpha}, \quad \mathbf{r} := \frac{\partial \tilde{\mathbf{u}}}{\partial \alpha}, \quad \mathbf{w} := \frac{\partial \hat{\mathbf{u}}}{\partial \alpha}, \quad \phi := \frac{\partial p}{\partial \alpha}, \quad \psi := \frac{\partial \lambda}{\partial \alpha}.$$

By differentiating the model (8-11) (with indicator function given by (16)) with respect to α , we obtain:

$$\mathbf{s}_t + \mathbf{r} \cdot \nabla \mathbf{u} + \tilde{\mathbf{u}} \cdot \nabla \mathbf{s} + \nabla \phi - \nu \Delta \mathbf{s} = \mathbf{0} \quad \text{in } \Omega \times (0, T), \quad (24)$$

$$\nabla \cdot \mathbf{s} = 0 \quad \text{in } \Omega \times (0, T), \quad (25)$$

$$\begin{aligned} \nabla \psi - \alpha^2 \nabla \cdot [(2(\mathbf{u} - \hat{\mathbf{u}}) \cdot (\mathbf{s} - \mathbf{w})) \nabla \tilde{\mathbf{u}} + |\mathbf{u} - \hat{\mathbf{u}}|^2 \nabla \mathbf{r}] + \mathbf{r} - \mathbf{s} \\ = 2\alpha \nabla \cdot |\mathbf{u} - \hat{\mathbf{u}}|^2 \nabla \tilde{\mathbf{u}} \quad \text{in } \Omega \times (0, T), \end{aligned} \quad (26)$$

$$\nabla \cdot \mathbf{r} = 0 \quad \text{in } \Omega \times (0, T), \quad (27)$$

$$-\alpha^2 \Delta \mathbf{w} + \mathbf{w} - \mathbf{s} = 2\alpha \Delta \hat{\mathbf{u}} \quad \text{in } \Omega \times (0, T). \quad (28)$$

The latter equation follows from the fact that $\hat{\mathbf{u}} = F_H(\mathbf{u}) \Rightarrow \hat{\mathbf{u}} - \alpha^2 \Delta \hat{\mathbf{u}} = \mathbf{u}$. System (24-28) is supplemented with boundary conditions

$$\mathbf{s} = \mathbf{r} = \mathbf{w} = \mathbf{0} \quad \text{on } \Gamma_{in} \cup \Gamma_{wall} \times (0, T), \quad (29)$$

$$(\nu \nabla \mathbf{s} - \phi \mathbf{I}) \cdot \mathbf{n} = (\alpha^2 \nabla \mathbf{w}) \cdot \mathbf{n} = \mathbf{0} \quad \text{on } \Gamma_{out} \times (0, T), \quad (30)$$

$$\begin{aligned} (\alpha^2 [(2(\mathbf{u} - \hat{\mathbf{u}}) \cdot (\mathbf{s} - \mathbf{w})) \nabla \tilde{\mathbf{u}} + |\mathbf{u} - \hat{\mathbf{u}}|^2 \nabla \mathbf{r}] - \psi \mathbf{I}) \cdot \mathbf{n} \\ = -2\alpha \nabla \cdot |\mathbf{u} - \hat{\mathbf{u}}|^2 \nabla \tilde{\mathbf{u}} \quad \text{on } \Gamma_{out} \times (0, T), \end{aligned} \quad (31)$$

and initial condition $\mathbf{s} = \mathbf{0}$ in $\Omega \times \{0\}$.

For the Leray- α -NL sensitivity system (24-28), we are not able to establish a well-posedness result. This is due to the fact that the well-posedness of Leray- α -NL has not been proven yet. The major difficulty is the nonlinear filter, which would not provide the extra regularity of $\tilde{\mathbf{u}}$ from the regularity of \mathbf{u} , since $\mathbf{u} - \hat{\mathbf{u}}$ could be zero. Hence we would need to apply different techniques from the ones used for the classical Leray- α model. We leave this study for a separate work. For now, we conjecture that Leray- α -NL, and its associated sensitivity system is well-posed for sufficiently smooth data.

3 Discrete schemes for the Leray- α and Leray- α -NL models and associated sensitivity systems

Let $\Delta t > 0$, $t^n = n\Delta t$, with $n = 0, \dots, M$ and $T = M\Delta t$. Moreover, we denote by y^n the approximation of a generic quantity y at the time t^n . For the time discretization, we adopt Backward Differentiation Formula of order 2 (BDF2, see e.g. [35]).

We assume \mathcal{T}_h to be a regular, conforming triangulation (tetrahedralization), with maximum element diameter h . The velocity and pressure finite element spaces $(X^h, Q^h) \subset (H^1(\Omega)^d, L^2(\Omega))$ are assumed to be LBB stable, i.e. it holds that

$$\inf_{q_h \in Q_h} \sup_{\mathbf{v}_h \in X_h} \frac{(\nabla \cdot \mathbf{v}_h, q_h)}{\|\nabla \mathbf{v}_h\| \|q_h\|} \geq \beta,$$

with β independent of h . Taylor-Hood elements (P_k, P_{k-1}) with $k \geq 2$ on triangles and tetrahedra are popular examples of LBB stable pairs [9, 26]. The usual modifications of these spaces can be made when non-homogeneous Dirichlet boundary conditions are imposed on the velocity.

Finally, we introduce the skew-symmetric form of the nonlinear term in the NSE is given by

$$b^*(\mathbf{u}, \mathbf{v}, \mathbf{w}) := \frac{1}{2}(\mathbf{u} \cdot \nabla \mathbf{v}, \mathbf{w}) - \frac{1}{2}(\mathbf{u} \cdot \nabla \mathbf{w}, \mathbf{v}), \quad \text{with } \mathbf{u}, \mathbf{v}, \mathbf{w} \in H^1(\Omega)^d.$$

If $\nabla \cdot \mathbf{u} = 0$, then $b^*(\mathbf{u}, \mathbf{v}, \mathbf{w}) = (\mathbf{u} \cdot \nabla \mathbf{v}, \mathbf{w})$. An important property of this operator is that $b^*(\mathbf{u}, \mathbf{v}, \mathbf{v}) = 0$ even if $\nabla \cdot \mathbf{u} \neq 0$, which can occur in discretizations.

For simplicity, when analyzing the discrete schemes we will consider wall-bounded flows, i.e. homogeneous Dirichlet conditions on all the boundary. The analyses that follow can be promptly adapted to fit the case of other boundary conditions.

Remark 1. The use of the skew-symmetric form of the nonlinearity is for analysis purposes only, and in our computations we use the usual convective formulation. In general, on sufficiently fine discretizations, very little difference between solutions from these formulations is observed. In practice, particularly in the case of zero traction outflow boundary conditions, the usual convective form is much more commonly used (since the skew-symmetric form requires a nonlinear boundary integral be incorporated into the formulation).

3.1 Discrete scheme for Leray- α

Given $T, \Delta t, \alpha > 0$, $\mathbf{f} \in L^\infty(0, T; H^{-1}(\Omega)^d)$, and $\mathbf{u}_h^0, \mathbf{u}_h^1 \in X_h$, we propose the following decoupled finite element discretization for the Leray- α model (1-4) with an implicit-explicit (also called semi-implicit) treatment of the nonlinear term:

Algorithm 3.1 For $n = 1, \dots, M-1$, given $\mathbf{u}_h^n, \mathbf{u}_h^{n-1}, \bar{\mathbf{u}}_h^n, \bar{\mathbf{u}}_h^{n-1} \in X_h$ find $\mathbf{u}_h^{n+1}, \bar{\mathbf{u}}_h^{n+1} \in X_h$ and $p_h^{n+1}, \lambda_h^{n+1} \in Q_h$ satisfying:

$$\begin{aligned} \frac{1}{2\Delta t} (3\mathbf{u}_h^{n+1} - 4\mathbf{u}_h^n + \mathbf{u}_h^{n-1}, \mathbf{v}_h) + b^*(2\bar{\mathbf{u}}_h^n - \bar{\mathbf{u}}_h^{n-1}, \mathbf{u}_h^{n+1}, \mathbf{v}_h) \\ - (p_h^{n+1}, \nabla \cdot \mathbf{v}_h) + \nu (\nabla \mathbf{u}_h^{n+1}, \nabla \mathbf{v}_h) = (\mathbf{f}(t^{n+1}), \mathbf{v}_h), \end{aligned} \quad (32)$$

$$(\nabla \cdot \mathbf{u}_h^{n+1}, q_h) = 0, \quad (33)$$

$$-(\lambda_h, \nabla \cdot \mathbf{z}_h) + \alpha^2 (\nabla \bar{\mathbf{u}}_h^{n+1}, \nabla \mathbf{z}_h) + (\bar{\mathbf{u}}_h^{n+1}, \mathbf{z}_h) = (\mathbf{u}_h^{n+1}, \mathbf{z}_h), \quad (34)$$

$$(\nabla \cdot \bar{\mathbf{u}}_h^{n+1}, \eta_h) = 0, \quad (35)$$

for every $\mathbf{v}_h, \mathbf{z}_h \in X_h$ and $q_h, \eta_h \in \times Q_h$.

Algorithm 3.1 decouples the filtering from the mass/momentum system. It is a straightforward extension of the analysis in [8] (for a linearized Crank-Nicolson temporal discretization with inf-sup stable finite elements) to prove that Algorithm 3.1 is unconditionally stable with respect to the time step size:

$$\|\mathbf{u}_h^M\|^2 + \nu \Delta t \sum_{n=2}^M \|\nabla \mathbf{u}_h^n\|^2 \leq C(\mathbf{u}_h^0, \mathbf{u}_h^1, \nu^{-1}, \mathbf{f}, \Omega). \quad (36)$$

Moreover, it converges optimally (under the usual smoothness assumptions) to the Leray- α solution in the following sense: if Taylor-Hood elements are used, then

$$\|\mathbf{u}(T) - \mathbf{u}_h^M\|^2 + \nu \Delta t \sum_{n=2}^M \|\nabla(\mathbf{u}(t^n) - \mathbf{u}_h^n)\|^2 \leq C(\Delta t^4 + h^{2k}). \quad (37)$$

We propose an analogous algorithm for the sensitivity system. At each time step, after solving the Leray- α discrete system we approximate the solution of sensitivity equation (17-20) as follows. We take $\mathbf{s}_h^0 = \mathbf{s}_h^1 = \mathbf{0}$. For $n = 1, \dots, M-1$, given $\mathbf{s}_h^n, \mathbf{s}_h^{n-1}, \mathbf{r}_h^n, \bar{\mathbf{r}}_h^{n-1} \in X_h$ we find $\mathbf{s}_h^{n+1}, \mathbf{r}_h^{n+1} \in X_h$ and $\phi_h^{n+1}, \psi_h^{n+1} \in Q_h$ satisfying

$$\begin{aligned} \frac{1}{2\Delta t} (3\mathbf{s}_h^{n+1} - 4\mathbf{s}_h^n + \mathbf{s}_h^{n-1}, \mathbf{v}_h) + b^*(2\bar{\mathbf{u}}_h^n - \bar{\mathbf{u}}_h^{n-1}, \mathbf{s}_h^{n+1}, \mathbf{v}_h) \\ - (\phi_h^{n+1}, \nabla \cdot \mathbf{v}_h) + \nu (\nabla \mathbf{s}_h^{n+1}, \nabla \mathbf{v}_h) = -b^*(2\mathbf{r}_h^n - \mathbf{r}_h^{n-1}, \mathbf{u}_h^{n+1}, \mathbf{v}_h), \end{aligned} \quad (38)$$

$$(\nabla \cdot \mathbf{s}_h^{n+1}, q_h) = 0, \quad (39)$$

$$-(\psi_h^{n+1}, \nabla \cdot \mathbf{z}_h) + \alpha^2 (\nabla \mathbf{r}_h^{n+1}, \nabla \mathbf{z}_h) + (\mathbf{r}_h^{n+1}, \mathbf{z}_h) = (\mathbf{s}_h^{n+1}, \mathbf{z}_h) - 2\alpha (\nabla \bar{\mathbf{u}}_h^{n+1}, \nabla \mathbf{z}_h), \quad (40)$$

$$(\nabla \cdot \mathbf{r}_h^{n+1}, \eta_h) = 0, \quad (41)$$

for all $\mathbf{v}_h, \mathbf{z}_h \in X_h$ and $q_h, \eta_h \in \times Q_h$.

Remark 2. The discrete sensitivity system (38-41) can be solved efficiently. In fact, system (38,39) is decoupled from (40,41). Furthermore, at each time step the linear

system arising from (38-41) has exactly the same matrix as system (32-35) allowing for the reusing of the preconditioner.

The following lemma proves that the discrete sensitivity system for the Leray- α model is stable with respect to the time step size under a mild restriction on the mesh size relative to the time step.

Lemma 2. *The discrete sensitivity system (38-41) with $(X_h, Q_h) = (P_k, P_{k-1})$ is stable provided the mesh size h and time step Δt are chosen to satisfy $\Delta t^3 \leq ch \leq \Delta t^{\frac{1}{2k-2}}$. Then we have*

$$\|\mathbf{s}_h^M\|^2 + \nu \Delta t \sum_{n=2}^M \|\nabla \mathbf{s}_h^{n+1}\|^2 \leq C,$$

where, C depends only on the problem data.

Proof. We take $\mathbf{v}_h = \mathbf{s}_h^{n+1}$ and $q_h = \phi_h^{n+1}$ in (38-39) and get that

$$\begin{aligned} \frac{1}{2\Delta t} (\|\mathbf{s}_h^{n+1}\|^2 - \|\mathbf{s}_h^n\|^2 + \|2\mathbf{s}_h^{n+1} - \mathbf{s}_h^n\|^2 - \|2\mathbf{s}_h^n - \mathbf{s}_h^{n-1}\|^2 + \|\mathbf{s}_h^{n+1} - 2\mathbf{s}_h^n + \mathbf{s}_h^{n-1}\|^2) \\ + \nu \|\nabla \mathbf{s}_h^{n+1}\|^2 = -b^*(2\mathbf{r}_h^n - \mathbf{r}_h^{n-1}, \mathbf{u}_h^{n+1}, \mathbf{s}_h^{n+1}). \end{aligned}$$

Let $\mathbf{e}_\mathbf{u}^{n+1} := \mathbf{u}_h^{n+1} - \mathbf{u}(t^{n+1})$. The right hand side term is handled by first adding and subtracting the true solution $\mathbf{u}(t^{n+1})$ to \mathbf{u}_h^{n+1} , then using Holder's inequality, and Sobolev embeddings to obtain

$$\begin{aligned} |b^*(2\mathbf{r}_h^n - \mathbf{r}_h^{n-1}, \mathbf{u}_h^{n+1}, \mathbf{s}_h^{n+1})| \\ \leq |b^*(2\mathbf{r}_h^n - \mathbf{r}_h^{n-1}, \mathbf{u}(t^{n+1}), \mathbf{s}_h^{n+1})| + |b^*(2\mathbf{r}_h^n - \mathbf{r}_h^{n-1}, \mathbf{e}_\mathbf{u}^{n+1}, \mathbf{s}_h^{n+1})| \\ \leq C \|2\mathbf{r}_h^n - \mathbf{r}_h^{n-1}\| (\|\mathbf{u}(t^{n+1})\|_{L^\infty} + \|\nabla \mathbf{u}(t^{n+1})\|_{L^3}) \|\nabla \mathbf{s}_h^{n+1}\| \\ + C \|2\mathbf{r}_h^n - \mathbf{r}_h^{n-1}\| (\|\mathbf{e}_\mathbf{u}^{n+1}\|_{L^\infty} + \|\nabla \mathbf{e}_\mathbf{u}^{n+1}\|_{L^3}) \|\nabla \mathbf{s}_h^{n+1}\|. \quad (42) \end{aligned}$$

By the assumed smoothness of the true solution, the first term is bounded by

$$\begin{aligned} C \|2\mathbf{r}_h^n - \mathbf{r}_h^{n-1}\| (\|\mathbf{u}(t^{n+1})\|_{L^\infty} + \|\nabla \mathbf{u}(t^{n+1})\|_{L^3}) \|\nabla \mathbf{s}_h^{n+1}\| \\ \leq \frac{\nu}{2} \|\nabla \mathbf{s}_h^{n+1}\|^2 + C \nu^{-1} \|2\mathbf{r}_h^n - \mathbf{r}_h^{n-1}\|^2. \end{aligned}$$

Thanks to the generalized inverse inequality (see, e.g. [9]), and well-known interpolation theory, we bound the second term as

$$\begin{aligned} C \|2\mathbf{r}_h^n - \mathbf{r}_h^{n-1}\| (\|\mathbf{e}_\mathbf{u}^{n+1}\|_{L^\infty} + \|\nabla \mathbf{e}_\mathbf{u}^{n+1}\|_{L^3}) \|\nabla \mathbf{s}_h^{n+1}\| \\ \leq \frac{\nu}{2} \|\nabla \mathbf{s}_h^{n+1}\|^2 + C \nu^{-1} h^{-1} \|\nabla \mathbf{e}_\mathbf{u}^{n+1}\|^2 \|2\mathbf{r}_h^n - \mathbf{r}_h^{n-1}\|^2. \end{aligned}$$

Combining the bounds and summing over n yields

$$\begin{aligned}
& \|s_h^M\|^2 + \|2s_h^M - s_h^{M-1}\|^2 + \nu \Delta t \sum_{n=2}^M \|\nabla s_h^{n+1}\|^2 \\
& \leq C \nu^{-1} \Delta t \sum_{n=2}^{M-1} \|2r_h^n - r_h^{n-1}\|^2 (1 + h^{-1} \|\nabla \mathbf{e}_u^{n+1}\|^2). \quad (43)
\end{aligned}$$

Next, we use equations (40,41) along with Cauchy-Schwarz and Young's inequalities to reveal

$$\alpha^2 \|\nabla(2r_h^n - r_h^{n-1})\|^2 + \|2r_h^n - r_h^{n-1}\|^2 \leq \|2s_h^n - s_h^{n-1}\|^2 + 4 \|\nabla(2\bar{\mathbf{u}}_h^n - \bar{\mathbf{u}}_h^{n-1})\|^2.$$

Combining this with (43) gives

$$\begin{aligned}
& \|s_h^M\|^2 + \|2s_h^M - s_h^{M-1}\|^2 + \nu \Delta t \sum_{n=2}^M \|\nabla s_h^{n+1}\|^2 \\
& \leq C \nu^{-1} \Delta t \sum_{n=2}^{M-1} \|2s_h^n - s_h^{n-1}\|^2 (1 + h^{-1} \|\nabla \mathbf{e}_u^{n+1}\|^2) \\
& \quad + C \nu^{-1} \Delta t \sum_{n=2}^{M-1} \|\nabla(2\bar{\mathbf{u}}_h^n - \bar{\mathbf{u}}_h^{n-1})\|^2 (1 + h^{-1} \|\nabla \mathbf{e}_u^{n+1}\|^2). \quad (44)
\end{aligned}$$

Using the convergence result (37), we have that

$$h^{-1} \|\nabla \mathbf{e}_u^{n+1}\|^2 \leq C \Delta t^{-1} h^{-1} (\Delta t^4 + h^{2k}) = C \left(\frac{\Delta t^3}{h} + \frac{h^{2k-1}}{\Delta t} \right).$$

Inserting this bound into (44) and applying the discrete Gronwall inequality (see e.g. [24]) gives the stated result. We note that there is no s_h^M on the right hand side. Thus there is no time step restriction associated with the discrete Gronwall inequality. \square

3.2 Discrete scheme for Leray- α -NL

Given $T, \Delta t, \alpha > 0$, $\mathbf{f} \in L^\infty(0, T; H^{-1}(\Omega)^d)$, and $\mathbf{u}_h^0, \mathbf{u}_h^1 \in X_h$, we propose the following decoupled finite element discretization for the Leray- α -NL model (8-11) with indicator function given by (16) and an implicit-explicit treatment of the nonlinear term:

Algorithm 3.2 For $n = 1, \dots, M-1$ find $\mathbf{u}_h^n, \tilde{\mathbf{u}}_h^n, \hat{\mathbf{u}}_h^n \in X_h$ and $p_h^n, \lambda_h^n \in Q_h$ satisfying:

$$\frac{1}{2\Delta t} (3\mathbf{u}_h^{n+1} - 4\mathbf{u}_h^n + \mathbf{u}_h^{n-1}, \mathbf{v}_h) + b^*(2\tilde{\mathbf{u}}_h^n - \tilde{\mathbf{u}}_h^{n-1}, \mathbf{u}_h^{n+1}, \mathbf{v}_h) - (p_h^{n+1}, \nabla \cdot \mathbf{v}_h) + \nu (\nabla \mathbf{u}_h^{n+1}, \nabla \mathbf{v}_h) = (\mathbf{f}(t^{n+1}), \mathbf{v}_h), \quad (45)$$

$$(\nabla \cdot \mathbf{u}_h^{n+1}, q_h) = 0, \quad (46)$$

$$-(\lambda_h, \nabla \cdot \mathbf{z}_h) + \alpha^2 (|\mathbf{u}_h^{n+1} - \hat{\mathbf{u}}_h^{n+1}|^2 \nabla \tilde{\mathbf{u}}_h^{n+1}, \nabla \mathbf{z}_h) + (\tilde{\mathbf{u}}_h^{n+1}, \mathbf{z}_h) = (\mathbf{u}_h^{n+1}, \mathbf{z}_h), \quad (47)$$

$$(\nabla \cdot \tilde{\mathbf{u}}_h^{n+1}, \eta_h) = 0, \quad (48)$$

$$\alpha^2 (\nabla \hat{\mathbf{u}}_h^{n+1}, \nabla \mathbf{y}_h) + (\hat{\mathbf{u}}_h^{n+1}, \mathbf{y}_h) = (\mathbf{u}_h^{n+1}, \mathbf{y}_h), \quad (49)$$

for every $\mathbf{v}_h, \mathbf{z}_h, \mathbf{y}_h \in X_h$ and $q_h, \eta_h \in Q_h$.

Note that the $\hat{\mathbf{u}}_h^n, \tilde{\mathbf{u}}_h^n$ velocities for $n = 0, 1$ can be determined from equations (47-49), since \mathbf{u}_h^0 and \mathbf{u}_h^1 are given.

Algorithm 3.2 efficiently decouples the mass/momentum system from the two filters. First, system (45,46) is solved for $\mathbf{u}_h^{n+1}, p_h^{n+1}$, then equation (49) is solved for $\hat{\mathbf{u}}_h^{n+1}$, and finally equations (47-48) are solved for $\tilde{\mathbf{u}}_h^{n+1}, \lambda_h^{n+1}$.

Algorithm 3.2 was studied in [6] with the only difference that the $|\mathbf{u}_h^{n+1} - \hat{\mathbf{u}}_h^{n+1}|$ in (47) term was not squared. This change does not affect the stability result proven in [6], which states

$$\|\mathbf{u}_h^M\|^2 + \nu \Delta t \sum_{n=2}^M \|\nabla \mathbf{u}_h^n\|^2 \leq C(\mathbf{u}_h^0, \mathbf{u}_h^1, \nu^{-1}, f, \Omega), \quad (50)$$

$$\|\hat{\mathbf{u}}_h^n\| \leq \|\mathbf{u}_h^n\|, \quad \|\nabla \hat{\mathbf{u}}_h^n\| \leq \|\nabla \mathbf{u}_h^n\|, \quad \|\tilde{\mathbf{u}}_h^n\| \leq \|\mathbf{u}_h^n\| \quad \text{for } 0 \leq n \leq M. \quad (51)$$

It is known from [8, 7] that the scheme (45-49) converges to a smooth Navier-Stokes solution \mathbf{u}_{NSE} as $h, \Delta t$, and α tends to 0. If Taylor-Hood elements are used, we have:

$$\|\mathbf{u}_{NSE}(T) - \mathbf{u}_h^M\|^2 + \nu \Delta t \sum_{n=2}^M \|\nabla(\mathbf{u}_{NSE}(t^n) - \mathbf{u}_h^n)\|^2 \leq C(\Delta t^4 + h^{2k} + \alpha^4). \quad (52)$$

At each time step, after solving the Leray- α -NL discrete system we approximate the solution of sensitivity equation (24-27) as follows. We take $\mathbf{s}_h^0 = \mathbf{s}_h^1 = \mathbf{0}$. For $n = 1, \dots, M-1$, given $\mathbf{s}_h^n, \mathbf{s}_h^{n-1}, \mathbf{r}_h^n, \bar{\mathbf{r}}_h^{n-1} \in X_h$ we find $\mathbf{s}_h^{n+1}, \mathbf{r}_h^{n+1}, \mathbf{w}_h^{n+1} \in X_h$ and $\phi_h^{n+1}, \psi_h^{n+1} \in Q_h$ satisfying:

$$\begin{aligned} & \frac{1}{2\Delta t} (3\mathbf{s}_h^{n+1} - 4\mathbf{s}_h^n + \mathbf{s}_h^{n-1}, \mathbf{v}_h) + b^* (2\tilde{\mathbf{u}}_h^n - \tilde{\mathbf{u}}_h^{n-1}, \mathbf{s}_h^{n+1}, \mathbf{v}_h) - (\phi_h^{n+1}, \nabla \cdot \mathbf{v}_h) \\ & + \nu (\nabla \mathbf{s}_h^{n+1}, \nabla \mathbf{v}_h) = -b^* (2\mathbf{r}_h^n - \mathbf{r}_h^{n-1}, \mathbf{u}_h^{n+1}, \mathbf{v}_h), \end{aligned} \quad (53)$$

$$(\nabla \cdot \mathbf{s}_h^{n+1}, q_h) = 0, \quad (54)$$

$$\begin{aligned} & \alpha^2 (|\mathbf{u}_h^{n+1} - \hat{\mathbf{u}}_h^{n+1}|^2 \nabla \mathbf{r}_h^{n+1}, \nabla \mathbf{z}_h) - (\psi_h^{n+1}, \nabla \cdot \mathbf{z}_h) + (\mathbf{r}_h^{n+1}, \mathbf{z}_h) \\ & = -2\alpha^2 ((\mathbf{u}_h^{n+1} - \hat{\mathbf{u}}_h^{n+1}) \cdot (\mathbf{s}_h^{n+1} - \mathbf{w}_h^{n+1})) \nabla \tilde{\mathbf{u}}_h^{n+1}, \nabla \mathbf{z}_h \\ & + (\mathbf{s}_h^{n+1}, \mathbf{z}_h) - 2\alpha (|\mathbf{u}_h^{n+1} - \hat{\mathbf{u}}_h^{n+1}|^2 \nabla \tilde{\mathbf{u}}_h^{n+1}, \nabla \mathbf{z}_h), \end{aligned} \quad (55)$$

$$(\nabla \cdot \mathbf{r}_h^{n+1}, \eta_h) = 0, \quad (56)$$

$$\alpha^2 (\nabla \mathbf{w}_h^{n+1}, \nabla \mathbf{y}_h) + (\mathbf{w}_h^{n+1}, \mathbf{y}_h) = (\mathbf{s}_h^{n+1}, \mathbf{y}_h), \quad (57)$$

for all $\mathbf{v}_h, \mathbf{z}_h, \mathbf{y}_h \in X_h$ and $q_h, \eta_h \in Q_h$.

This scheme can also be efficiently computed. In fact, system (53,54) is computed first, followed by system (57) and (55,56). Moreover, the matrices for the linear systems are exactly the same as for (45-49).

Theorem 2. *The discrete sensitivity scheme is stable (53-57): for all $\Delta t > 0$ we have*

$$\|\mathbf{s}_h^M\|^2 + \nu \Delta t \sum_{n=1}^M \|\nabla \mathbf{s}_h^n\|^2 \leq C(\mathbf{u}, \nu^{-1}, T), \quad (58)$$

and for any n

$$2\alpha^2 \|\nabla \mathbf{w}_h^n\|^2 + \|\mathbf{w}_h^n\|^2 \leq \|\mathbf{s}_h^n\|^2, \quad \|\mathbf{r}_h^n\| \leq \|\mathbf{s}_h^n\|.$$

Proof. By taking $\mathbf{v}_h = \mathbf{s}_h^{n+1}$ in (53) and $q_h = \phi_h^{n+1}$ in (54) along with Holder's inequality and Sobolev embedding theorems, we get

$$\begin{aligned} & \frac{1}{4\Delta t} (\|\mathbf{s}_h^{n+1}\|^2 - \|\mathbf{s}_h^n\|^2 + \|2\mathbf{s}_h^{n+1} - \mathbf{s}_h^n\|^2 - \|2\mathbf{s}_h^n - \mathbf{s}_h^{n-1}\|^2 + \|\mathbf{s}_h^{n+1} - 2\mathbf{s}_h^n + \mathbf{s}_h^{n-1}\|^2) \\ & \leq + \nu \|\nabla \mathbf{s}_h^{n+1}\|^2 C \|2\mathbf{r}_h^n - \mathbf{r}_h^{n-1}\| (\|\nabla \mathbf{u}_h^{n+1}\|_{L^3} + \|\mathbf{u}_h^{n+1}\|_{L^\infty}) \|\nabla \mathbf{s}_h^{n+1}\|. \end{aligned} \quad (59)$$

Young's inequality and the assumption of \mathbf{u}_h converging sufficiently fast yield:

$$\begin{aligned} & \frac{1}{2\Delta t} (\|\mathbf{s}_h^{n+1}\|^2 - \|\mathbf{s}_h^n\|^2 + \|2\mathbf{s}_h^{n+1} - \mathbf{s}_h^n\|^2 - \|2\mathbf{s}_h^n - \mathbf{s}_h^{n-1}\|^2 + \|\mathbf{s}_h^{n+1} - 2\mathbf{s}_h^n + \mathbf{s}_h^{n-1}\|^2) \\ & \leq + \nu \|\nabla \mathbf{s}_h^{n+1}\|^2 C \nu^{-1} \|2\mathbf{r}_h^n - \mathbf{r}_h^{n-1}\|^2. \end{aligned} \quad (60)$$

Next, taking $\mathbf{y}_h = \mathbf{w}_h^{n+1}$ in (57) and $\mathbf{z}_h = \mathbf{r}_h^{n+1}$ in (55) provides

$$2\alpha^2 \|\nabla \mathbf{w}_h^{n+1}\|^2 + \|\mathbf{w}_h^{n+1}\|^2 \leq \|\mathbf{s}_h^{n+1}\|^2, \quad (61)$$

and

$$\begin{aligned}
& \alpha^2 \|\mathbf{u}_h^{n+1} - \hat{\mathbf{u}}_h^{n+1} | \nabla \mathbf{r}_h^{n+1} \|^2 + \|\mathbf{r}_h^{n+1}\|^2 = (\mathbf{s}_h^{n+1}, \mathbf{r}_h^{n+1}) \\
& - 2\alpha^2 ((\mathbf{u}_h^{n+1} - \hat{\mathbf{u}}_h^{n+1}) \cdot (\mathbf{s}_h^{n+1} - \mathbf{w}_h^{n+1})) \nabla \tilde{\mathbf{u}}_h^{n+1}, \nabla \mathbf{r}_h^{n+1}) \\
& - 2\alpha (|\mathbf{u}_h^{n+1} - \hat{\mathbf{u}}_h^{n+1}|^2 \nabla \tilde{\mathbf{u}}_h^{n+1}, \nabla \mathbf{r}_h^{n+1}).
\end{aligned}$$

Cauchy-Schwarz and Young's inequalities applied to each term on the right-hand side give the estimate

$$\begin{aligned}
& \alpha^2 \|\mathbf{u}_h^{n+1} - \hat{\mathbf{u}}_h^{n+1} | \nabla \mathbf{r}_h^{n+1} \|^2 + \|\mathbf{r}_h^{n+1}\|^2 \leq \\
& \|\mathbf{s}_h^{n+1}\|^2 + 8\alpha^2 \|\mathbf{s}_h^{n+1} - \mathbf{w}_h^{n+1} | \nabla \tilde{\mathbf{u}}_h^{n+1} \|^2 + 8\|\mathbf{u}_h^{n+1} - \hat{\mathbf{u}}_h^{n+1} | \nabla \tilde{\mathbf{u}}_h^{n+1} \|^2.
\end{aligned}$$

Assuming \mathbf{u}_h converges and using (61), we have that

$$\|\mathbf{r}_h^{n+1}\|^2 \leq \|\mathbf{s}_h^{n+1}\|^2 + C + C\alpha^2 \|\mathbf{s}_h^{n+1} - \mathbf{w}_h^{n+1}\|^2 \leq C(1 + \|\mathbf{s}_h^{n+1}\|^2). \quad (62)$$

Inequalities (62) in (60) yield:

$$\begin{aligned}
& \frac{1}{2\Delta t} (\|\mathbf{s}_h^{n+1}\|^2 - \|\mathbf{s}_h^n\|^2 + \|2\mathbf{s}_h^{n+1} - \mathbf{s}_h^n\|^2 - \|2\mathbf{s}_h^n - \mathbf{s}_h^{n-1}\|^2 + \|\mathbf{s}_h^{n+1} - 2\mathbf{s}_h^n + \mathbf{s}_h^{n-1}\|^2) \\
& + \nu \|\nabla \mathbf{s}_h^{n+1}\|^2 \leq C\nu^{-1} (\|\mathbf{s}_h^n\|^2 + \|\mathbf{s}_h^{n-1}\|^2). \quad (63)
\end{aligned}$$

To complete the proof we sum over n and apply Gronwall's inequality. There is no time step restriction since the power of \mathbf{s}_h on the right hand side is less than $n + 1$ [24]. \square

4 Numerical testing

In this section we compute solutions to the Leray- α and Leray- α -NL models, and associated sensitivities for two test problems. For both tests, we use Taylor-Hood elements, i.e. P_2 elements for velocities and relative sensitivities, and P_1 elements for pressures and Lagrange multipliers. The computations were performed using Freefem software [22].

4.1 Channel flow past a forward-backward step

We consider the two dimensional channel flow past a forward-backward step. The domain is a 40×10 rectangle, with a 1×1 step placed five units in. See Fig. 1. We impose boundary conditions (5-7) for the Leray- α model and (12-14) for the Leray- α -NL model with $\mathbf{u}_{in} = (y(10 - y)/25, 0)^T$. The boundary conditions for the sensitivity systems are as reported in Sec. 2. We set $\mathbf{f} = \mathbf{0}$ and $\nu = 1/600$. The correct physical behavior for a NSE solution is a smooth velocity profile, with eddies forming and detaching behind the step; see, e.g., [27, 20].

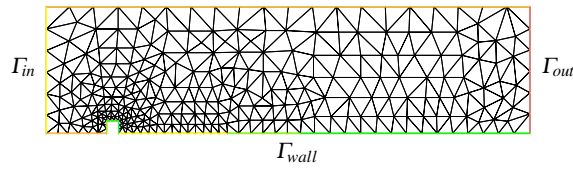


Fig. 1 Mesh used for the computations of the channel flow past a forward-backward step.

We consider a Delaunay triangulated mesh (shown in Fig. 1), with a total of 2,575 total degrees of freedom. The time step is set to $\Delta t = 0.1$. We let the simulations run until $T = 40$. We show in Fig. 2 the streamlines over velocity magnitude contours given by the Leray- α model with $\alpha = 0.25$ and $\alpha = 0.1$ at time $T = 40$. We observe the solutions are similar away from the step, but behind the step they exhibit very different behavior: for $\alpha = 0.25$ there is no eddy separation, while for $\alpha = 0.1$ the correct transient behavior of eddy shedding is predicted. This sensitivity to α near the step and lack of sensitivity away from the step are predicted in the plot of the velocity sensitivity magnitude $|\mathbf{s}_h|$ for $\alpha = 0.25$ reported in Fig. 3.

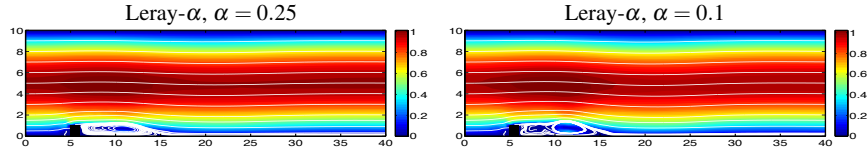


Fig. 2 Streamlines over velocity magnitude contours given by the Leray- α model with $\alpha = 0.25$ (left) and $\alpha = 0.1$ (right) at time $T = 40$.

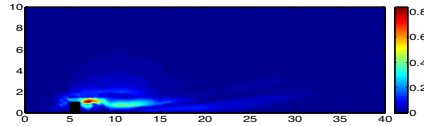


Fig. 3 Velocity sensitivity magnitude $|\mathbf{s}_h|$ for the Leray- α model with $\alpha = 0.25$ at time $T = 40$.

The same test was run with the Leray- α -NL model. Fig. 4 displays the streamlines over velocity magnitude contours given by the Leray- α -NL model with $\alpha = 0.25$ and $\alpha = 0.1$ at time $T = 40$. Here we observe that both solutions correctly predict eddy shedding behind the step. Moreover, we observe that the velocity sensitivity magnitude for $\alpha = 0.25$ shown in Fig. 5 is quite small. In fact even though $|\mathbf{s}_h|$ is largest behind the step, just as in the Leray- α case, for the nonlinear model the magnitude of sensitivity is almost 2 orders of magnitude smaller: at $T = 40$ $\|\mathbf{s}_h\|_{L^\infty} \approx 0.01$ for the Leray- α -NL model, while $\|\mathbf{s}_h\|_{L^\infty} \approx 0.80$ for the Leray- α model. Hence the Leray- α -NL correctly predicts the physical behavior with both

choices of α , and is much less sensitive to the parameter choice than the classical Leray- α model. Fig. 5 reports also the indicator function $a(\mathbf{u}_h) = |\mathbf{u}_h - \hat{\mathbf{u}}_h|^2$ for the Leray- α -NL model with $\alpha = 0.25$ at time $T = 40$. We see that the indicator function takes larger values in the region behind the step, as expected.

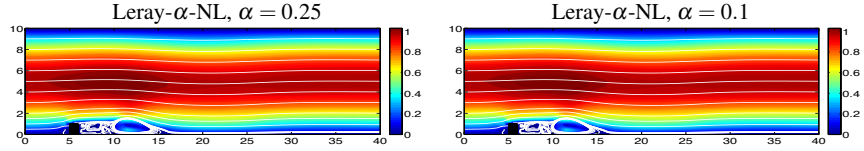


Fig. 4 Streamlines over velocity magnitude contours given by the Leray- α -NL model with $\alpha = 0.25$ (left) and $\alpha = 0.1$ (right) at time $T = 40$.

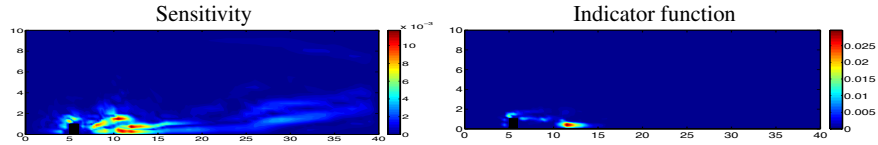


Fig. 5 Velocity sensitivity magnitude $|s_h|$ (left) and indicator function $a(\mathbf{u}_h) = |\mathbf{u}_h - \hat{\mathbf{u}}_h|^2$ (right) for the Leray- α -NL model with $\alpha = 0.25$ at time $T = 40$.

4.2 Channel flow with a contraction and two outlets

The second numerical test is taken from Heywood et. al. [25]: channel flow with a contraction, one inlet on the left side, and outlets at the top and right. We impose boundary conditions (5-7) for the Leray- α model and (12-14) for the Leray- α -NL model with $\mathbf{u}_{in} = (4y(1-y), 0)^T$. The boundary conditions for the sensitivity systems are as reported in Sec. 2. We set $\mathbf{f} = \mathbf{0}$, $\nu = 0.001$, and $\mathbf{u}_0 = \mathbf{0}$. We let the simulations run until $T = 4$. The Navier-Stokes velocity magnitude on a fully resolved mesh is shown in Fig. 7 for $T = 4$. This solution was obtained using a fully implicit Crank-Nicolson temporal discretization with time step of $\Delta t = 0.005$ and (P_3, P_2) grad-div stabilized Taylor-Hood elements on the triangular mesh with 260,378 total degrees of freedom.

We consider a coarse Delaunay generated triangulation (shown in Fig. 6), with a total of 24,553 total degrees of freedom, that is one order of magnitude less than a fully resolved mesh. Fig. 8 shows the velocity magnitude contours given by the Leray- α model with $\alpha = 0.16$ and $\alpha = 0.14$ at time $T = 4$. First of all, we note these solutions do not match well the solution given by DNS shown in Fig. 7. Comparing to each other, the solutions for $\alpha = 0.16$ and $\alpha = 0.14$ in Fig. 8 appear similar on

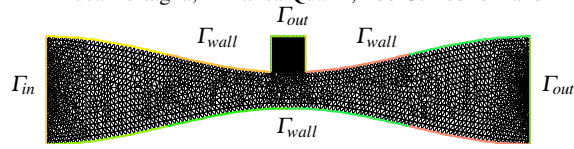


Fig. 6 Mesh used for the computations of the channel flow with a contraction and two outlets.

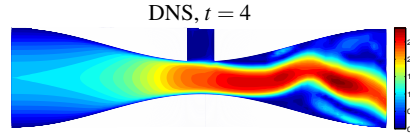


Fig. 7 Velocity magnitude contours given by DNS (NSE on a fully resolved mesh) at time $T = 4$.

the left half of the channel, but on the right hand side the ‘jet’ for $\alpha=0.14$ extends slightly farther. Also there are discrepancies near the top outlet; see zoomed-in views in Fig. 8. These differences are predicted by the velocity sensitivity solution for $\alpha = 0.16$ reported in Fig. 9.

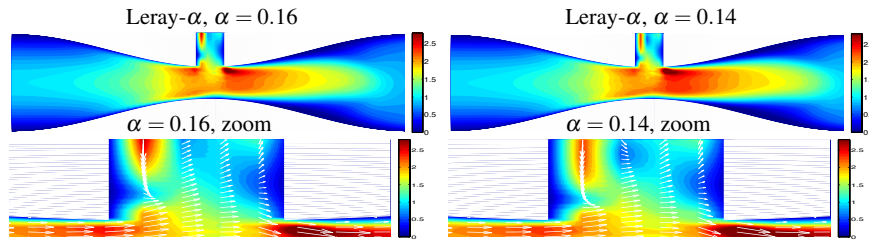


Fig. 8 Velocity magnitude contours given by the Leray- α model with $\alpha = 0.16$ (top left) and $\alpha = 0.14$ (top right) at time $T = 4$ and respective zoomed in views (bottom).

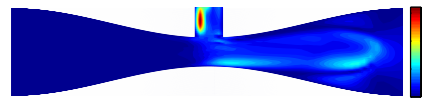


Fig. 9 Velocity sensitivity magnitude $|s_h|$ for the Leray- α model with $\alpha = 0.16$ at time $T = 4$ s.

The same test was run with Leray- α -NL. Fig. 10 displays the velocity magnitude contours given by the Leray- α -NL model with $\alpha = 0.16$ and $\alpha = 0.14$ at time $T = 4$. These solutions match each other well and match the general pattern of the solution given by DNS shown in Fig. 7. Examining the sensitivity solution for $\alpha = 0.16$ in Fig. 11 we see greater sensitivity near the top outlet. However, the velocity sensitivity magnitude $|s_h|$ is smaller than for the classical Leray- α model; compare Fig. 11

with Fig. 9. Also for this second test, the Leray- α -NL correctly predicts the physical behavior with both choices of α , and is less sensitive to the parameter choice than the classical Leray- α model. Finally, Fig. 11 reports also the indicator function $a(\mathbf{u}_h) = |\mathbf{u}_h - \hat{\mathbf{u}}_h|^2$ for the Leray- α -NL model with $\alpha = 0.16$ at time $T = 4$. Fig. 11 shows that it is a suitable indicator function since it correctly selects the regions of the domain where the velocity does need regularization.

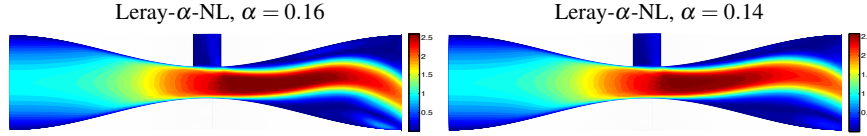


Fig. 10 Velocity magnitude contours given by the Leray- α -NL model with $\alpha = 0.16$ (left) and $\alpha = 0.14$ (right) at time $T = 4$.

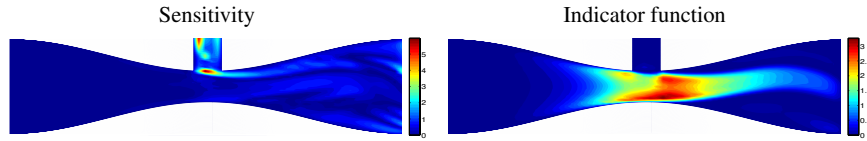


Fig. 11 Velocity sensitivity magnitude $|s_h|$ (left) and indicator function $a(\mathbf{u}_h) = |\mathbf{u}_h - \hat{\mathbf{u}}_h|^2$ (right) for the Leray- α -NL model with $\alpha = 0.16$ at time $T = 4$.

5 Conclusions

In this paper, we applied the sensitivity equation method to study the sensitivity to the filtering radius α of the classical Leray- α and a Leray model with a deconvolution-based indicator function, called Leray- α -NL. We proposed efficient and stable numerical schemes for the approximation of both models and their respective sensitivity systems, and we tested them on two benchmark problems. We showed that the velocity sensitivity magnitude correctly identifies the region of the domain where the velocity is sensitive to variations of α . Moreover, we showed that the Leray- α -NL model correctly predicts the physical solution for different values of α , and is much less sensitive to the parameter choice than the classical Leray- α model.

This is a preliminary work aiming at assessing numerical schemes for the sensitivity equations. Clearly, we expect to use the sensitivity results to perform specific strategies for the selection of the filter radius. This will be based on the following steps: (1) Compute the LES solution and the sensitivity with a conservative choice of the radius ($\alpha = \alpha_0$ “large”); (2) Rapidly recompute the solution for smaller values of α according to the expansion

$$\mathbf{u}(\boldsymbol{\alpha}) \approx \mathbf{u}(\boldsymbol{\alpha}_0) + \mathbf{s}(\boldsymbol{\alpha}_0)(\boldsymbol{\alpha} - \boldsymbol{\alpha}_0).$$

The definition of the appropriate criteria for the identification of the most appropriate radius is expected to be largely problem-dependent and will be subject of forthcoming works.

Acknowledgements The research presented in this work was carried out during LR's visit at the Department of Mathematics and Computer Science at Emory University in the fall semester 2014. This support is gratefully acknowledged. This research has been supported in part by the NSF under grants DMS-1620384/DMS-1620406 (Quaini and Veneziani), DMS-1262385 (Quaini), Emory URC Grant 2015 Numerical Methods for Flows at Moderate Reynolds Numbers in LVAD (Veneziani), and DMS-1522191 (Rebholz)

References

1. M. Anitescu and W. J. Layton. Sensitivities in large eddy simulation and improved estimates of turbulent flow functionals. *Journal of Computational Physics*, 178:391–426, 2001.
2. L. Bertagna, A. Quaini, and A. Veneziani. Deconvolution-based nonlinear filtering for incompressible flows at moderately large Reynolds numbers. *Int. J. Num. Meth. Fluids*, published online, 2016.
3. J. Borggaard and J. Burns. A sensitivity equation approach to shape optimization in fluid flows. In *Flow Control, volume 68 of Proceedings of the IMA*. Springer-Verlag, 1995.
4. J. Borggaard and J. Burns. A PDE sensitivity equation method for optimal aerodynamic design. *Journal of Computational Physics*, 136:366–384, 1997.
5. J. Borggaard and A. Verma. Solutions to continuous sensitivity equations using automatic differentiation. *SIAM Journal of Scientific Computing*, 22:39–62, 2001.
6. A. Bowers and L. Rebholz. Numerical study of a regularization model for incompressible flow with deconvolution-based adaptive nonlinear filtering. *Computer Methods in Applied Mechanics and Engineering*, 258:1–12, 2013.
7. A. Bowers, L. Rebholz, A. Takhirov, and C. Trenchea. Improved accuracy in regularization models of incompressible flow via adaptive nonlinear filtering. *International Journal for Numerical Methods in Fluids*, 70:805–828, 2012.
8. A. Bowers and L.G. Rebholz. Increasing accuracy and efficiency in FE computations of the Leray-deconvolution model. *Numerical Methods for Partial Differential Equations*, 28(2):720–736, 2012.
9. S. Brenner and L.R. Scott. *The Mathematical Theory of Finite Element Methods*. Springer-Verlag, 2008.
10. Y. Cao and E. Titi. On the rate of convergence of the two-dimensional α -models of turbulence to the Navier-Stokes equations. *Numerical Functional Analysis and Optimization*, 30:1231–1271, 2009.
11. A. Cheskidov, D. Holm, E. Olson, and E.S. Titi. On a Leray- α model of turbulence. *Proceedings of The Royal Society A*, 461:629–649, 2005.
12. A. Dunca and Y. Epshteyn. On the Stolz-Adams deconvolution model for the large-eddy simulation of turbulent flows. *SIAM J. Math. Anal.*, 37(6):1980–1902, 2005.
13. B. Geurts and D. Holm. Leray simulation of turbulent shear layers. In I. Castro and P. Hancock, editors, *Advances in Turbulence IX: Proceedings of the Ninth European Turbulence Conference*, pages 1–4. CIMNE, 2002.
14. B.J. Geurts and D. Holm. Regularization modeling for large eddy simulation. *Physics of Fluids*, 15:L13, 2003.

15. B.J. Geurts and D.D. Holm. Leray and LANS- α modelling of turbulent mixing. *Journal of Turbulence*, 7(10):1–33, 2006.
16. A. Godfrey and E. Cliff. Direct calculation of aerodynamic force derivatives: A sensitivity equation approach. *Proceedings of the 36th AIAA Aerospace Sciences Meeting and Exhibit, 0393*, 1998.
17. J. Graham, D. Holm, P. Mininni, and A. Pouquet. Three regularization models of the Navier-Stokes equations. *Physics of Fluids*, 20:–35107:1–15, 2008.
18. J.P. Graham, D. Holm, P. Mininni, and A. Pouquet. The effect of subfilter-scale physics on regularization models. *J. Sci. Comp*, 49(1):21–34, 2011.
19. B.J. Geurts, A. Kuczaj, and E. Titi. Regularization modeling for large-eddy simulation of homogeneous isotropic decaying turbulence. *Journal of Physics A: Math. Theor.*, 41:1–29, 2008.
20. M. Gunzburger. *Finite Element Methods for Viscous Incompressible Flow: A Guide to Theory, Practice, and Algorithms*. Academic Press, Boston, 1989.
21. M. Gunzburger. Sensitivities, adjoints and flow optimization. *Int. Jour. Num. Meth. Fluids*, 31:53–78, 1999.
22. F. Hecht. New development in freefem++. *J. Numer. Math.*, 20(3-4):251–265, 2012.
23. M. Hecht, D. Holm, M. Petersen, and B. Wingate. The LANS- α and Leray turbulence parameterizations in primitive equation ocean modeling. *Journal of Physics A: Math. Theor.*, 41:1–23, 2008.
24. J. Heywood and R. Rannacher. Finite element approximation of the nonstationary Navier-Stokes problem. Part IV: Error analysis for the second order time discretization. *SIAM J. Numer. Anal.*, 2:353–384, 1990.
25. J. Heywood, R. Rannacher, and S. Turek. Artificial boundaries and flux and pressure conditions for the incompressible Navier-Stokes equations. *International Journal for Numerical Methods in Fluids*, 22:325–352, 1996.
26. W. Layton. *An Introduction to the Numerical Analysis of Viscous Incompressible Flows*. SIAM, 2008.
27. W. Layton, C.C. Manica, M. Neda, and L.G. Rebholz. The joint helicity-energy cascade for homogeneous isotropic turbulence generated by approximate deconvolution models. *Advances and Applications in Fluid Mechanics*, 4:1–46, 2008.
28. W. Layton, N. Mays, M. Neda, and C. Trenchea. Numerical analysis of modular regularization methods for BDF2 time discretization of the Navier-Stokes equations. *ESAIM: Mathematical Modelling and Numerical Analysis*, 48:765–793, 2014.
29. W. Layton and L. Rebholz. *Approximate deconvolution models of turbulence: analysis, phenomenology, and numerical analysis*. Springer-Verlag, 2012.
30. W. Layton, L. Rebholz, and C. Trenchea. Modular nonlinear filter stabilization of methods for higher reynolds numbers flow. *Journal of Mathematical Fluid Mechanics*, 14:325–354, 2012.
31. J. Leray. Essai sur le mouvement d’un fluide visqueux emplissant l’espace. *Journal de Mathématiques Pures et Appliquées*, 63:193–248, 1934.
32. Y. Liu, P. Tucker, and R. Kerr. Linear and nonlinear model large eddy simulations of a plane jet. *Computers and Fluids*, 37:439–449, 2008.
33. E. Lunasin, S. Kurien, and E. Titi. Spectral scaling of the Leray- α model for two-dimensional turbulence. *Journal of Physics A: Math. Theor.*, 41:1–10, 2008.
34. F. Pahlevani. Sensitivity computations of eddy viscosity models with an application in drag computation. *International Journal for Numerical Methods in Fluids.*, 52(4):381–392, 2006.
35. A. Quarteroni, R. Sacco, and F. Saleri. *Numerical Mathematics*. Springer Verlag, 2007.
36. P. Sagaut and T.Lê. Some investigations of the sensitivity of large eddy simulation. *Tech. Rep., ONERA*, 1997.
37. L. Stanley and D. Stewart. *Design sensitivity analysis: Computational issues of sensitivity equation methods*. Frontiers in Mathematics. SIAM, Philadelphia, 2002.
38. R. Verstappen. On restraining the production of small scales of motion in a turbulent channel flow. *Computers and Fluids*, 37:887–897, 2008.